

Thirty-eight-negative kinase 1 mediates trauma-induced intestinal injury and multi-organ failure

Milena Armacki,¹ Anna Katharina Trugenberg,¹ Ann K. Ellwanger,¹ Tim Eiseler,¹ Christiane Schwerdt,² Lucas Bettac,¹ Dominik Langgartner,³ Ninel Azoitei,¹ Rebecca Halbgebauer,⁴ Rüdiger Groß,¹ Tabea Barth,¹ André Lechel,¹ Benjamin M. Walter,¹ Johann M. Kraus,⁵ Christoph Wiegrefe,⁶ Johannes Grimm,⁷ Annika Scheffold,⁸ Marlon R. Schneider,⁹ Kenneth Peuker,¹⁰ Sebastian Zeißig,¹⁰ Stefan Britsch,⁶ Stefan Rose-John,¹¹ Sabine Vettorazzi,¹² Eckhart Wolf,⁹ Andrea Tannapfel,¹³ Konrad Steinestel,¹⁴ Stefan O. Reber,³ Paul Walther,¹⁵ Hans A. Kestler,⁵ Peter Radermacher,¹⁶ Thomas F.E. Barth,⁷ Markus Huber-Lang,⁴ Alexander Kleger,¹ and Thomas Seufferlein¹

¹Department of Internal Medicine I, University Hospital Ulm, Ulm, Germany. ²Waldkrankenhaus "Rudolph Elle" Eisenberg, Lehrstuhl für Orthopädie Uniklinik Jena, Jena, Germany. ³Laboratory for Molecular Psychosomatics, Clinic for Psychosomatic Medicine and Psychotherapy, and ⁴Institute of Clinical and Experimental Trauma Immunology, University Hospital Ulm, Ulm, Germany. ⁵Institute of Medical Systems Biology and ⁶Institute of Molecular and Cellular Anatomy, Ulm University, Ulm, Germany. ⁷Institute of Pathology and ⁸Department of Internal Medicine III, University Hospital Ulm, Ulm, Germany. ⁹Gene Center, LMU Munich, Munich, Germany. ¹⁰Center for Regenerative Therapies Dresden, TU Dresden, Dresden, Germany. ¹¹Institute of Biochemistry, CA University Kiel, Kiel, Germany. ¹²Institute of Comparative Molecular Endocrinology, Ulm University, Ulm, Germany. ¹³Institute of Pathology, Ruhr University Bochum, Bochum, Germany. ¹⁴Institute of Pathology and Molecular Pathology, Bundeswehrkrankenhaus Ulm, Ulm, Germany. ¹⁵Central Facility for Electron Microscopy, University of Ulm, Ulm, Germany. ¹⁶Institute of Anesthesiological Pathophysiology and Process Engineering, Ulm University, Ulm, Germany.

Dysregulated intestinal epithelial apoptosis initiates gut injury, alters the intestinal barrier, and can facilitate bacterial translocation leading to a systemic inflammatory response syndrome (SIRS) and/or multi-organ dysfunction syndrome (MODS). A variety of gastrointestinal disorders, including inflammatory bowel disease, have been linked to intestinal apoptosis. Similarly, intestinal hyperpermeability and gut failure occur in critically ill patients, putting the gut at the center of SIRS pathology. Regulation of apoptosis and immune-modulatory functions have been ascribed to Thirty-eight-negative kinase 1 (TNK1), whose activity is regulated merely by expression. We investigated the effect of TNK1 on intestinal integrity and its role in MODS. TNK1 expression induced crypt-specific apoptosis, leading to bacterial translocation, subsequent septic shock, and early death. Mechanistically, TNK1 expression in vivo resulted in STAT3 phosphorylation, nuclear translocation of p65, and release of IL-6 and TNF- α . A TNF- α neutralizing antibody partially blocked development of intestinal damage. Conversely, gut-specific deletion of TNK1 protected the intestinal mucosa from experimental colitis and prevented cytokine release in the gut. Finally, TNK1 was found to be deregulated in the gut in murine and porcine trauma models and human inflammatory bowel disease. Thus, TNK1 might be a target during MODS to prevent damage in several organs, notably the gut.

Introduction

Disturbance of gut integrity has been proposed to drive systemic inflammatory response syndrome (SIRS) and to promote multiple organ failure (MOF). Balanced homeostasis in the gut is critically regulated by 3 closely interrelated entities: the epithelium, the immune system, and the microbiome. Distant organ damage frequently follows cytokine and endotoxin release from the gut, a finding that has established the gut as an origin of sepsis and MOF (1). In line with this finding, gut permeability is increased after severe tissue trauma, in different forms of shock and also in critically ill patients in intensive care units. Increased gut per-

meability can therefore also be used as an early marker for the development of MOF (1). In this context, enhanced gut permeability can be induced by inappropriate intestinal apoptosis (2). The disturbed barrier sustains an inflammatory environment and, in turn, can lead to alterations in the virulence of the microbiome, an observation that has been termed acute gastrointestinal injury (AGI) (3). Besides the gut, the liver and lungs are also frequently affected during SIRS and MOF (4–6). Recent evidence shows that the mechanisms that first lead to intestinal injury also induce the release of nonbacterial proinflammatory signals and factors that cause distant tissue damage. Thus, gut-derived factors might indirectly contribute to SIRS and subsequent MOF (1, 6). Hence, it appears reasonable that a common molecular event can mediate the damage at each respective site. For instance, Fas ligand, a known inducer of apoptosis, was found to be highly expressed in both AGI (7) and acute lung injury (8). This observation suggests that an organ-spanning factor might exist that initiates apoptosis during MOF. Notably, apoptosis is essential not only during MOF but also for the pathogenesis of a variety of non-SIRS-related gastrointestinal disorders (9) such as ischemia/reperfusion injury,

► Related Commentary: p. 4764

Authorship note: AK and TS contributed equally to this work.

Conflict of interest: The authors have declared that no conflict of interest exists.

License: Copyright 2018, American Society for Clinical Investigation.

Submitted: October 6, 2017; **Accepted:** August 28, 2018.

Reference information: *J Clin Invest.* 2018;128(11):5056–5072.

<https://doi.org/10.1172/JCI97912>.

necrotizing colitis (10) in infants, infectious diarrhea, celiac disease (11), and chronic inflammatory bowel disease (IBD) (12).

One of the hallmarks of AGI and inflammatory gastrointestinal disorders is the excessive production of proinflammatory cytokines, e.g., TNF- α , which promotes the massive tissue damage in the gut and distant organs (5, 13). Intestinal epithelial cells have been described as a source of IL-6 upon stimulation with proinflammatory cytokines, e.g., TNF- α (14). Finally, it has been shown that TNF- α peaks with maximum intestinal injury frequently occurring upon liver transplantation (15) and also sustains chronic inflammation in IBD. Anti-TNF- α antibodies have become a mainstay in IBD treatment. Therapeutic neutralization of TNF- α not only limits the inflammation but also improves intestinal barrier function and has an impact on apoptosis of mucosal immune cells and the formation of regulatory macrophages, as well as other immune-modulating properties. Similar features can be found in AGI. Despite all this knowledge, the factors mediating the damage in the intestinal tract during AGI, IBD, and SIRS are only partly understood.

Here, we propose Thirty-eight-negative kinase 1 (TNK1) as a critical mediator of intestinal apoptosis and subsequent organ failure. TNK1 is a member of the ACK family of kinases initially isolated from CD34⁺Lin⁻CD38⁻ stem/progenitor cells (16). Its transcripts can be detected in many fetal tissues, including the gastrointestinal tract (ref. 16 and our unpublished data), but in only a few adult tissues, including prostate, testis, ovary, small intestine, and colon (17). TNK1 expression was also detected in leukemia and pancreatic cancer cell lines. Data suggest a not-well-studied role of TNK1 in the differentiation of the gastrointestinal tract, in particular in the small and the large intestine but also in some tumors (18, 19). Expression of this kinase appears to be tightly regulated in adult tissues. Examination of the murine *Tnk1* promoter revealed that cellular stress reverses the otherwise strong repression of the *Tnk1* promoter and induces TNK1 expression through increased high-affinity interactions between the nuclear proteins SP1, SP3, AP2, and MED1 (20). Once expressed, the kinase shows maximum catalytic activity. Interestingly, there are no known physiological activators that can further increase the activity of the kinase. This feature of TNK1 activity could explain why its expression is so tightly regulated. TNK1 can exert both tumor suppressor and oncogenic activities (19, 21–23). It can downregulate RAS activity (24), and *Tnk1*-knockout mice have been reported to develop tumors (19). Interestingly, TNK1 expression/activity enables TNF- α -induced apoptosis (17).

Here, we identify TNK1 as a potent mediator of intestinal apoptosis that in turn disturbs intestinal barrier function, leading to induced MOF of gut origin. Conversely, deletion of TNK1 from the intestinal epithelium protects mice from inflammation-induced injury.

Results

A TNK1 gain-of-function mouse model. Under physiological conditions, TNK1 is expressed at low levels in few adult tissues, including the intestine, and its expression determines its catalytic activity. To analyze the effect of TNK1 expression in vivo, we established a mouse model with doxycycline-inducible expression of TNK1 using a previously described Cre-flox-based, inducible cassette exchange system (ref. 25 and Figure 1A). The doxycycline-inducible locus expresses best in proliferating cells, while it does not

express well in postmitotic cells (Michael Kyba, personal communication). Initially, we examined transgene expression across various organs. Before induction, TNK1 expression was hardly detectable in most of the organs examined but could be readily induced upon application of doxycycline (Supplemental Figure 1, A–C; supplemental material available online with this article; <https://doi.org/10.1172/JCI97912DS1>). After 12 hours of induction, we observed a homogeneous expression of the transgene along the crypt-villus axis in the small and large intestine and minor expression in the liver (data not shown). Twenty-four hours after the start of doxycycline treatment there was a maximum TNK1 expression in the gut, but only patchy expression in the pancreas, liver (Supplemental Figure 1, A–C), and bone marrow (Supplemental Figure 1D). Notably, staining against the Myc tag and the TNK1 protein using a polyclonal antibody showed an identical pattern of TNK1 expression along crypts in the small intestine and colon. Since the Myc tag antibody detects only recombinant, tagged protein, there is no immunostaining in control mice. The polyclonal TNK1 antibody detects not only the basal physiological level of TNK1 in sham mice but also an increase of TNK1 expression in response to doxycycline treatment (Supplemental Figure 1A). TNK1 expression was not detectable in the lungs, kidney, brain or heart (Supplemental Figure 1B).

Expression of TNK1 causes severe distress. The first remarkable observation in TNK1-expressing mice was a substantial change in their locomotor activity (LMA) (26). Within the first 24 hours after induction of TNK1, the mice exhibited a significant decrease in their LMA (total distance) compared with saline-treated mice (Figure 1B). Altered LMA was particularly pronounced during the nocturnal, active phase, when control mice exhibited their peak activity. This observation was accompanied by decreased intake of food and a drop in body weight by 10%–15% (Figure 1, C and D). Also, we observed hypothermia in TNK1-expressing mice with an average core body temperature of 28°C, 24 hours after doxycycline treatment (Figure 1E). Hypothermia is a hallmark of stress and is also indicative of sepsis in mice (27). In line with this, mice also showed a significant drop in plasma glucose levels and an increase in plasma corticosterone (Figure 1F). Moreover, total and differential leukocyte counts implied a systemic bacterial inflammation; there was a significant increase in the total number of white blood cells and the absolute numbers of granulocytes and monocytes (Figure 1G). This and the slightly decreased proportion of lymphocytes of the whole white blood cell count indicated bacterial inflammation (Figure 1G). TNK1-expressing mice also exhibited anemia as demonstrated by a reduced number of circulating red blood cells and a decrease of both hemoglobin and hematocrit values (Figure 1H). Notably, the hematological changes observed were not due to an adverse effect of doxycycline or a result of the TNK1 expression in bone marrow cells (Supplemental Figure 1E and Supplemental Figure 2, A and B). Various factors contribute to the development of anemia, including blood loss, increased erythrocyte destruction, e.g., during sepsis, and impaired red blood cell synthesis. However, all these systemic alterations present in TNK1-expressing mice can occur during a SIRS (27).

TNK1-expressing mice exhibit a coagulation disorder and early death. In patients with SIRS, changes in biomarkers of coagulation or fibrinolysis leading to hypercoagulopathy, as well as low

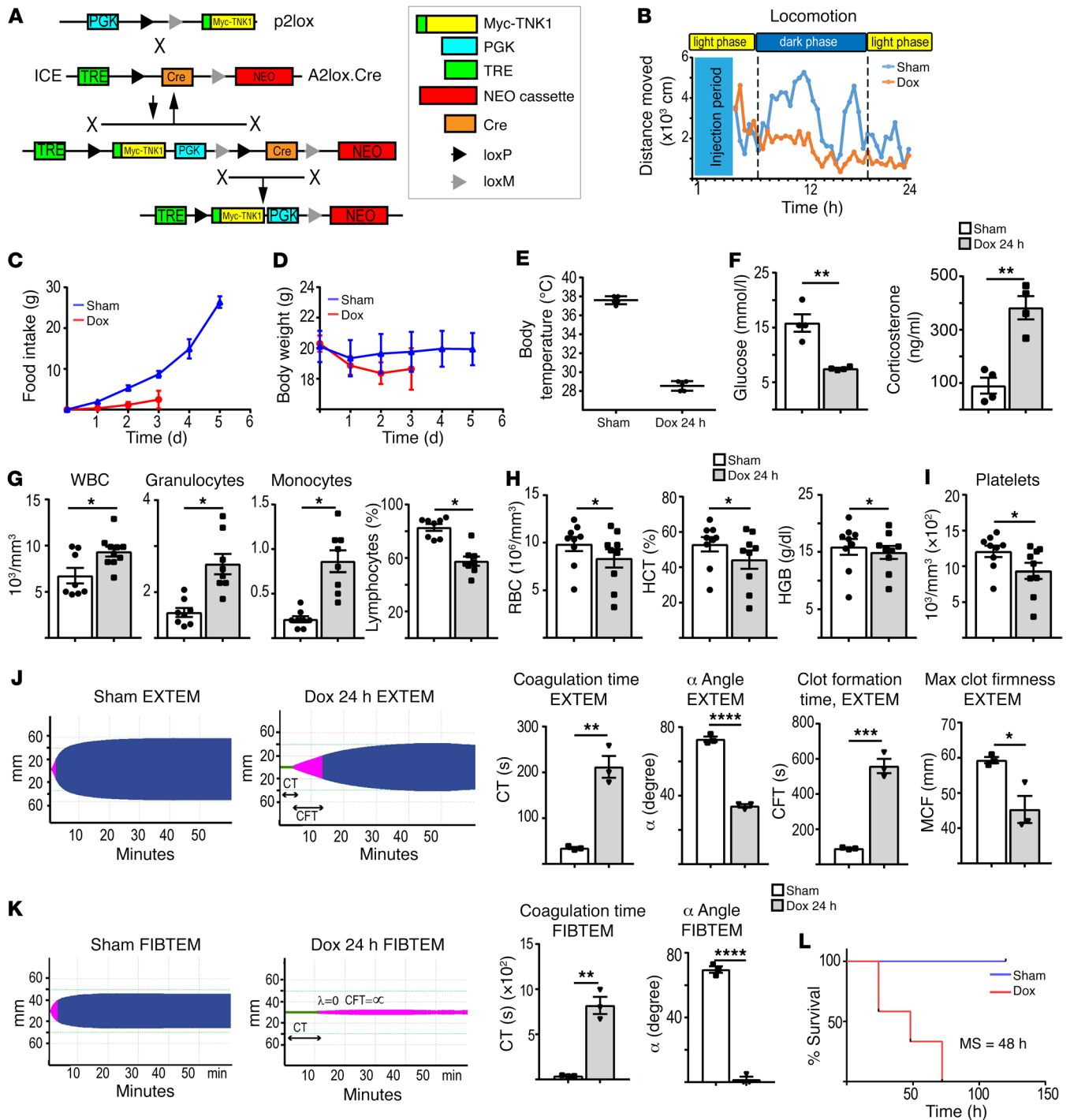


Figure 1. Expression of TNK1 causes animal distress, systemic inflammation, and rapid lethality. (A) By an inducible cassette exchange (ICE) approach (60), Myc-tagged Tnk1 was targeted to a specific conditionally regulated locus by Cre-lox recombination. (B) Behavior analysis shows that expression of TNK1 impairs locomotion of the animals ($n = 6$ per group). (C and D) TNK1-expressing mice show signs of cachexia, as demonstrated by decreased food intake (C) and body weight (D) ($n = 12$ per group, $t = 24$ hours). (E) Mice exhibit a drop in body temperature upon TNK1 expression ($n = 5$ per group, $t = 24$ hours). (F) TNK-expressing mice exhibit hypoglycemia (left) and hypercortisolism (right) ($n = 4$ per group). (G) Differential blood count suggests systemic bacterial inflammation ($n = 8-10$ per group, $t = 24$ hours), as designated by an increase in the total number of white blood cells (WBC), granulocytes, and monocytes and a decrease of lymphocytes. (H) TNK1-expressing mice show a significant decrease in red blood cell (RBC) number, declined hematocrit (HCT), and hemoglobin (HGB). (I-K) TNK1-expressing mice also exhibit a dysregulation of coagulation, as indicated by diminished platelets ($n = 9$ per group) (I) and rotational thromboelastometry analysis ($n = 3-4$ per group) (J and K) ($t = 24$ hours). Prolonged EXTEM (J) and FIBTEM (K) clotting time (CT) and reduced α angle specify abnormal clot formation. A prolonged EXTEM clot formation time (CFT) and reduced EXTEM maximum clot firmness (MCF) indicate abnormal clot formation in TNK1-expressing mice (J, right 2 graphs). (L) Kaplan-Meier analysis shows decreased survival upon TNK1 expression ($n = 12$). MS, median survival. Data are expressed as mean \pm SEM. Differences were tested by parametric 2-tailed, unpaired Student's t tests ($*P = 0.01-0.05$; $**P = 0.001-0.01$; $***P = 0.0001-0.001$; $****P < 0.0001$).

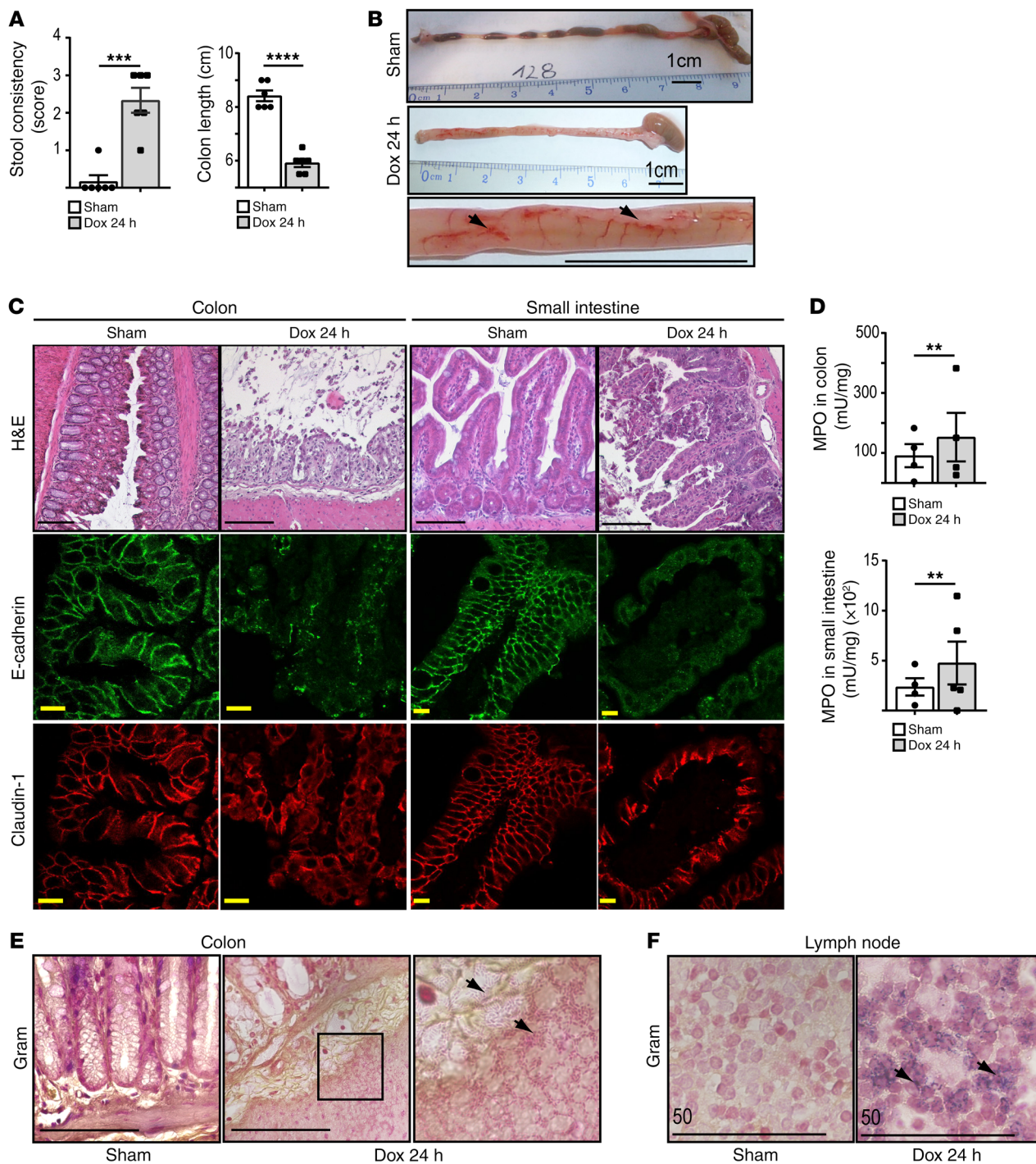


Figure 2. TNK1 expression impairs the functionality of the intestinal barrier. (A and B) TNK1-expressing mice show bloody diarrhea and significant colon shrinkage (A) and erythema (B, arrows) 24 hours after doxycycline administration ($n = 6$ per group). Macroscopically the colon also appears distended. (C) Expression of TNK1 perturbs normal intestinal architecture. Mice show severe disruption of the mucosal architecture in small and large intestine. Representative histological images of the large and small intestine of *Rosa26rtTA/+*, *Hrpt Myc-Tnk1tg* 24 hours after doxycycline or saline administration are shown. Expression of TNK1 affects the integrity of both adherens junctions and tight junctions as demonstrated by a substantial reduction in E-cadherin (middle panels) and claudin-1 (bottom panels) immunoreactivity in the epithelium of the small and large intestine of TNK1-expressing animals. (D) Myeloperoxidase (MPO) elevation in gut tissues of TNK1-expressing mice points to neutrophil infiltration. Neutrophil accumulation contributes to local tissue destruction ($n = 4$ per group). (E and F) Impairment of intestinal barrier is accompanied by bacterial translocation to the intestinal wall (E) and to the mesenteric lymph nodes (F) (arrows indicate Gram⁺ bacteria). Data are expressed as mean \pm SEM. Differences were tested by parametric 2-tailed, unpaired Student's t tests (** $P = 0.001-0.01$; **** $P = 0.0001-0.001$; ***** $P < 0.0001$). Scale bars: 50 μm (F); 100 μm (C and E); 10 μm (IF images).

platelet counts, are frequently detectable and correlate with organ dysfunction. TNK1-expressing mice exhibited a decreased platelet count (Figure 1I). Coagulopathy in SIRS becomes evident by a procoagulant and antifibrinolytic state, which predisposes to microvascular thrombosis, tissue ischemia, and organ hypoperfusion (28). Closer examination of the coagulation system in TNK1-expressing mice revealed a massive dysregulation of blood coagulation. The clotting time (CT) was significantly prolonged. The α angle as a readout for platelet function was significantly decreased in TNK1-expressing mice as compared with control mice (Figure 1J). A prolonged EXTEM clot formation time and reduced EXTEM maximum clot firmness (MCF) indicated abnormal clot formation in TNK1-expressing mice (Figure 1J). Additionally, reduced EXTEM MCF indicated a deficiency of clottable substrate (fibrinogen and/or platelets). Indeed, TNK1-expressing mice also exhibited a fibrinogen deficiency as assessed by FIBTEM analysis (Figure 1, J and K). The FIBTEM test measures the formation of a fibrin clot after inhibition of platelet function. TNK1-expressing mice showed a prolonged FIBTEM CT and a FIBTEM α angle equal to zero (Figure 1K).

The combination of hypothermia, cachexia, a decrease in clottable substrates, anemia, and leukocytosis suggested a septic process. In agreement with this notion, the majority of animals died rapidly after induction of TNK1. Kaplan-Meier analysis revealed a median overall survival of only 48 hours upon induction of TNK1 by doxycycline (Figure 1L).

Expression of TNK1 induces disruption of the epithelial barrier. Next, we were interested in the potential cause(s) of systemic inflammation and rapid lethality in TNK1-expressing mice. The most prominent clinical findings in these mice were diarrhea and bloody stools (Figure 2A and Supplemental Table 2). Macroscopic examination of the colon revealed a significant shortening of the colon by 25% as well as intestinal hyperemia (Figure 2, A and B). At the microscopic level, we observed a massive shedding of enterocytes into the lumen and severe disruption of the colonic mucosal architecture (Figure 2C). There was also a substantial cell exfoliation into the lumen of the small intestine, leading to shortening and blunting of the villi (Figure 2C). In line with these findings, expression and distribution of the adherens junction (AJ) component E-cadherin and the tight junction (TJ) marker claudin-1 were both strongly reduced and disorganized in TNK1-expressing mice (Figure 2C). AJs and TJs are critical for maintenance of the intestinal barrier (29). Doxycycline dosing did not contribute to the pathological phenotype in the intestine; WT mice (C57BL/6J) maintained the normal intestinal architecture (Supplemental Figure 2C). The severity of the gut damage correlated with accumulation/activation of neutrophils as indicated by a significant increase of the neutrophil activation marker myeloperoxidase in the gut of TNK1-expressing mice (Figure 2D). Thus, expression of TNK1 resulted in a massive breakdown of the intestinal barrier and consequently the loss of the defense mechanisms against luminal toxins, antigens, and enteric bacteria. This prompted us to seek a putative bacterial translocation as a consequence of the breakdown of the epithelial barrier. Indeed, Gram staining demonstrated bacteria within the intestinal epithelial layers (Figure 2E) as well as in mesenteric lymph nodes (Figure 2F) of TNK1-expressing mice, but not of control littermates. Thus, TNK1-expressing mice

encounter a massive breakdown of the intestinal epithelial barrier, resulting in bacterial translocation, SIRS, and ultimately death.

TNK1 induces apoptosis predominantly at the intestinal crypts. Next, we were interested in the mechanisms that caused the rapid damage of the intestinal epithelium. Since TNK1 has been shown to induce apoptosis of certain cell types (17), we examined whether apoptosis could be the driving force of intestinal damage in our model. We measured mRNA expression of antiapoptotic (*Xiap*, *Bcl2*, and *Mcl1*) and proapoptotic (*Bax*, *Bad*, *Bak*, and *Bcl2l1* [*Bim*]) genes, respectively. Interestingly, both marker sets were upregulated in the small and large intestine of TNK1-expressing animals (Figure 3, A–C, and Supplemental Figure 3, A and B).

To determine the net effect of these marker gene alterations, we assessed the protein levels of relevant apoptosis effectors by Western blotting. We could detect increased levels of cleaved caspase-3 (cC3) and cleaved PARP (cPARP) in the gut of TNK1-overexpressing mice, indicating induction of apoptosis (Figure 3D). To determine where the apoptotic cells were distributed along the crypt-villus axis in our mouse model, we performed immunostaining for cC3 and counted the positive cells at the respective positions (30). Intriguingly, there were significantly more apoptotic cells in crypts than at the villi (Figure 3, E and F). Immunostaining for the Myc-tagged TNK1 in doxycycline-treated mice excluded that the distribution of cC3-positive cells was merely due to spatial variations in the expression levels of the TNK1 transgene (Supplemental Figure 1D).

Ablation of the stem cell compartment impairs regeneration and allows intestinal failure. Intestinal stem cells reside at the crypt basis and give rise to differentiated progeny (31, 32). We were interested in whether the stem cell compartment is more vulnerable to TNK1-driven signals that potentially compromise the regenerative capacity of the intestinal epithelium. Indeed, transcript of the stem cell marker *Lgr5* was markedly reduced in the gut of TNK1-expressing mice compared with sham-treated counterparts (Figure 3G). Consistently, cC3 immunostaining revealed positive cells at crypt positions reported to be the pools of *Lgr5*⁺ and position +4 stem cells (Figure 3H, top panels). Notably, position +4 stem cells have been described as a reserved stem cell pool necessary for regeneration in the absence of *Lgr5*⁺ cells after widespread intestinal apoptosis to prevent intestinal failure (33, 34).

Extensive intestinal apoptosis disables an adequate regenerative response, resulting in gastrointestinal failure (34). Therefore, we evaluated the number of regenerating crypts, defined as crypt-like structures that contain at least 5 adjacent Ki67⁺ proliferating cells (Figure 3H) (34). In WT epithelium, proliferating cells were uniformly distributed in every crypt (Figure 3I). In contrast, in TNK1-expressing animals, regenerating crypts were barely detectable, indicating strongly impaired regeneration (Figure 3, H and I). There were patches of Ki67⁺ crypts scattered throughout the epithelium, with large unstained areas in regions lacking crypts, and scarce Ki67⁺ cells in a few residual crypts (Supplemental Figure 3C). In line with these data, the number of differentiated goblet cells was also diminished upon TNK1 induction (Supplemental Figure 3, C and D).

Thus, TNK1-mediated apoptosis leads to ablation of the intestinal stem cell pool and thereby prevents adequate repopulation of the intestine. This effect is likely to be primarily responsible for the

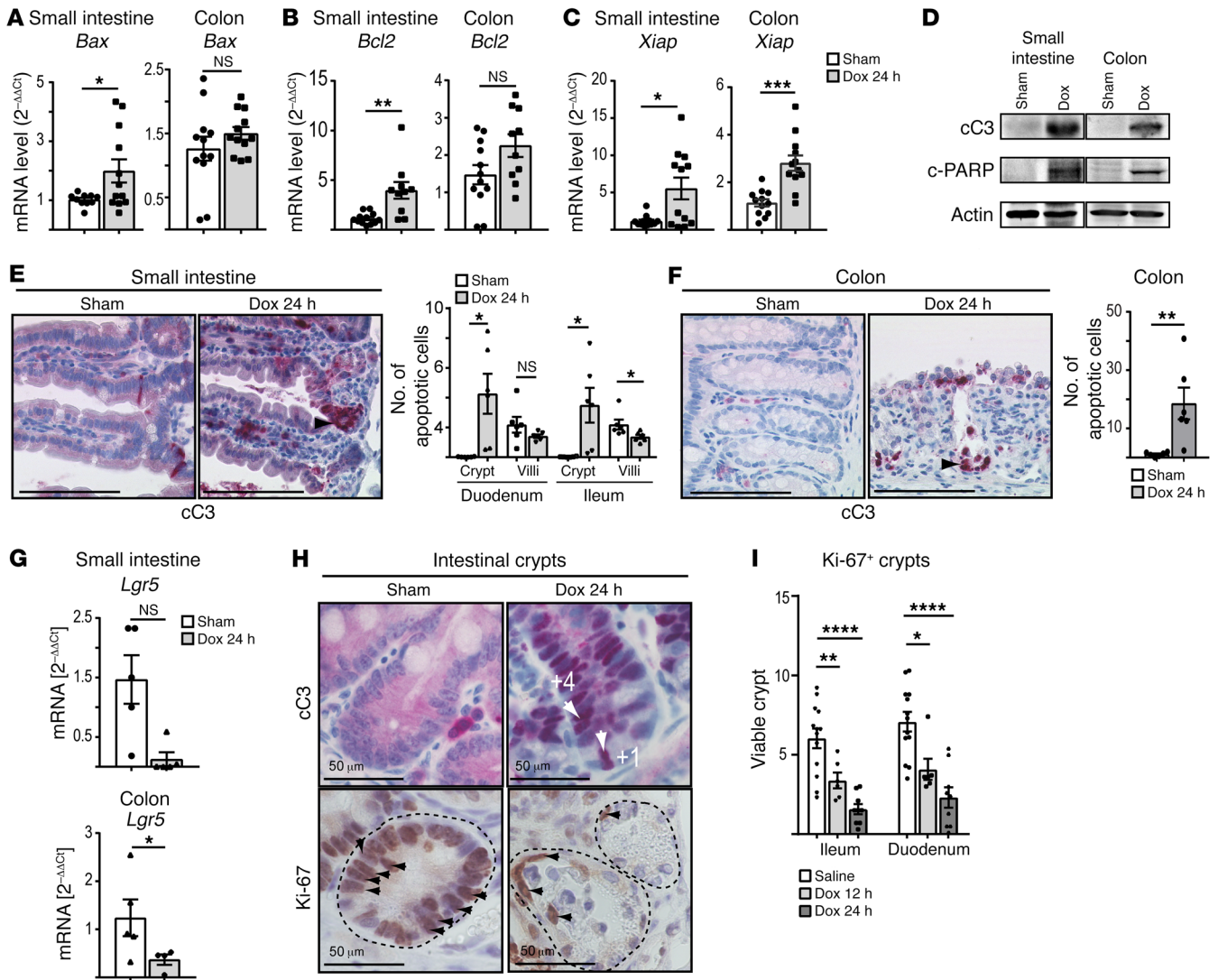


Figure 3. Mice with forced TNK1 expression show massive apoptosis at the base of the intestinal crypts. (A–C) Graphs display elevated mRNA levels of proapoptotic (*Bax*) and prosurvival (*Xiap*, *Bcl2*) genes in the small and large intestine ($n = 10$ per group) of TNK1-expressing mice. (D) Western blots show expression of cC3 and its substrate cPARP in the small intestine and colon ($n = 3$). (E and F) Representative images of the murine small and large intestine show immunoreactivity for the apoptotic marker cC3 (arrowheads point to cC3-positive cells). Corresponding charts depict positional quantification of apoptosis ($n = 6$ per group), which was done according to Buczaccki et al. (61) by counting of cells at the crypt (stem cell compartment) and villi. Cells were counted at the base of the crypt (from positions 0 to +4, counting from the bottom of the crypt to the transit-amplifying progenitor cells and the villus area). (G) Expression of the stem cell marker LGR5 in the small and large intestine is also reduced in *Tnk1*-expressing mice as indicated by quantitative reverse transcriptase PCR (RT-qPCR) analysis ($n = 5$ per group). (H) Representative images of the crypt-base stem cell compartment positive for cC3 (top panel: white arrows indicate stem and reserve stem [position +4] cells positive for apoptotic marker) or the Ki67 proliferative marker (bottom panel). (I) Crypt phenotype was quantified by counting of regenerating crypts, which are defined as containing at least 5 adjacent Ki67⁺ cells (arrows) contained within a crypt-like structure (34) ($n = 10$ –12 per group). All analyses were performed 24 hours after doxycycline or saline treatment. Data are expressed as mean \pm SEM. Differences were tested by parametric 2-tailed, unpaired Student's *t* tests. ANOVA test was applied for multiple-comparison analysis. The mean of each column was compared with the mean of a control column by Dunnett's multiple-comparisons test. (* $P = 0.01$ –0.05; ** $P = 0.001$ –0.01; *** $P = 0.0001$ –0.001; **** $P < 0.0001$). Scale bars: 50 (H); 100 μ m (E and F).

intestinal failure as the primary cause of wasting and death of the TNK1-expressing animals.

TNK1-induced damage primarily affects the intestine. High TNK1 expression in the intestinal epithelium could explain the observed clinical phenotype. However, we were interested in whether there was additional damage to other organs in TNK1-expressing animals. Liver, lung, and pancreas of TNK1-expressing mice exhibited anatomical and histological changes. The Histology Activity Index

grading system for chronic hepatitis (35, 36) was applied to assess necroinflammatory activity in the liver. Although TNK1 expression in the liver was already detectable 12 hours after doxycycline, gross and histopathological examination exhibited no major differences between TNK1-expressing and control mice. Only minor inflammation, as shown by foci of infiltrating leukocytes, was detectable 12 hours after doxycycline exposure (data not shown). However, 24 hours after doxycycline exposure, livers of TNK1-expressing

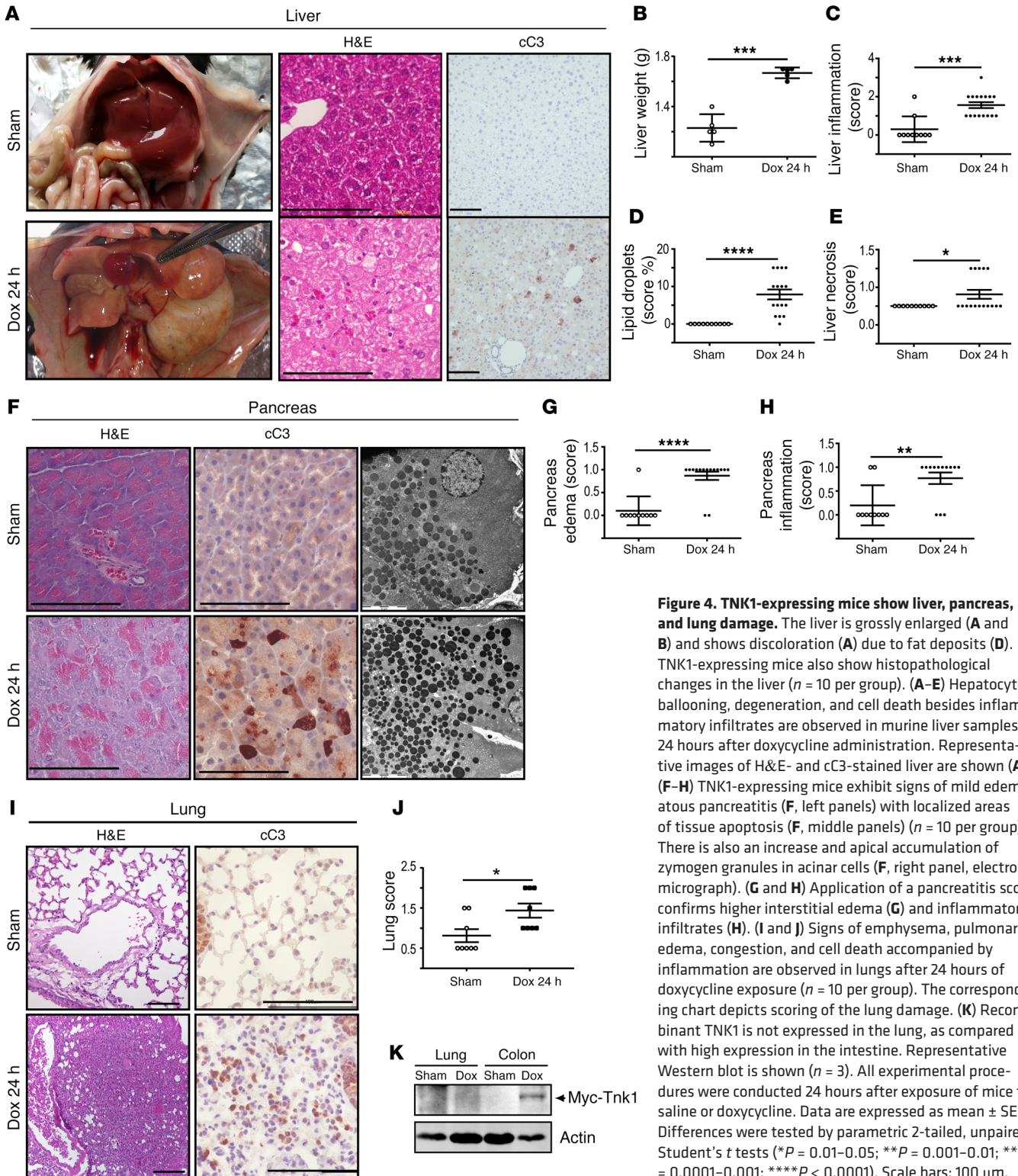


Figure 4. TNK1-expressing mice show liver, pancreas, and lung damage. The liver is grossly enlarged (A and B) and shows discoloration (A) due to fat deposits (D). TNK1-expressing mice also show histopathological changes in the liver ($n = 10$ per group). (A–E) Hepatocyte ballooning, degeneration, and cell death besides inflammatory infiltrates are observed in murine liver samples 24 hours after doxycycline administration. Representative images of H&E- and cC3-stained liver are shown (A). (F–H) TNK1-expressing mice exhibit signs of mild edematous pancreatitis (F, left panels) with localized areas of tissue apoptosis (F, middle panels) ($n = 10$ per group). There is also an increase and apical accumulation of zymogen granules in acinar cells (F, right panel, electron micrograph). (G and H) Application of a pancreatitis score confirms higher interstitial edema (G) and inflammatory infiltrates (H). (I and J) Signs of emphysema, pulmonary edema, congestion, and cell death accompanied by inflammation are observed in lungs after 24 hours of doxycycline exposure ($n = 10$ per group). The corresponding chart depicts scoring of the lung damage. (K) Recombinant TNK1 is not expressed in the lung, as compared with high expression in the intestine. Representative Western blot is shown ($n = 3$). All experimental procedures were conducted 24 hours after exposure of mice to saline or doxycycline. Data are expressed as mean \pm SEM. Differences were tested by parametric 2-tailed, unpaired Student's t tests (* $P = 0.01$ – 0.05 ; ** $P = 0.001$ – 0.01 ; *** $P = 0.0001$ – 0.001 ; **** $P < 0.0001$). Scale bars: 100 μ m.

mice exhibited signs of mild hepatitis without necrosis (Figure 4, A–E) accompanied by an increase in liver weight (Figure 4B). Similar kinetics of damage was observed in the pancreas of the TNK1-expressing mice. Here we detected mild edematous, non-necrotic pancreatitis (Figure 4, F–H). Damage in pancreas and liver were only detectable in TNK1-expressing animals. However, the overall

number of cC3-positive cells in the liver and pancreas was far lower in comparison with the intestine (Figure 3, E and F, and Figure 4, A and H). In contrast to liver and pancreas, TNK1 was virtually not expressed in the lung (Figure 4K), although visible histopathological changes were present in the lung. We detected alveolar collapse, thickening of the alveolar membranes, and protein debris in

the airspace together with alveolar edema, bronchial destruction, and apoptosis, all pointing to acute lung injury (Figure 4, I-K).

Different mechanistic scenarios could explain these observations: (a) organs other than the gut are less permissive to a TNK1-driven apoptotic program; (b) alternatively, the TNK1 expression threshold that drives catastrophic damage is not reached in pancreas and liver because of differences in the absolute transgene expression levels (Supplemental Figure 1, C and D); (c) and/or indirect mechanisms potentiate damage at distant organs, e.g., lung, as suggested by the absence of the TNK1 transgene via immunoblotting. Taken together, TNK1 expression appears as a critical module in mediating tissue damage primarily in the gut.

TNK1 expression is dysregulated in response to stress across various species. Since TNK1 expression can be induced by cell stress (20), we wanted to define a potential pathophysiological role of TNK1 in the course of trauma. First, we examined whether TNK1 expression would change in response to various severe traumatic stressors using a mouse model of experimental trauma. Anesthetized mice were subjected to a sham procedure or polytrauma in the presence or absence of an additional hemorrhagic shock as described previously (37). TNK1 transcripts were significantly increased in the small intestine and colon already 4 hours after trauma induction (Figure 5A). A minor increase could also be detected in the lung and pancreas (Figure 5B), while *Tnk1* expression levels in liver and kidney remained unchanged (data not shown). Hemorrhagic shock in addition to the polytrauma further increased *Tnk1* expression in small intestine and pancreas (Figure 5, A and B). Immunohistochemistry for TNK1 confirmed an increase in TNK1 expression in the small intestine and colon epithelia upon polytrauma and hemorrhagic shock (Figure 5C).

Our data from the TNK1-transgenic mice proposed an induction of SIRS followed by multi-organ dysfunction syndrome (MODS) and death due to a breakdown of the intestinal barrier, bacterial translocation, and sepsis, suggesting an underlying pathophysiological role of TNK1. Therefore, we next examined TNK1 expression in an experimental murine sepsis model, where sepsis is induced by cecal ligation and perforation (38). Using this model, we detected a significant increase in TNK1 expression at the protein and mRNA levels in the ileum of septic mice (Figure 5, D and E). To further corroborate these findings, we also used a porcine model (39) of experimental hemorrhagic trauma, since pigs are more representative of the human condition regarding physiology, anatomy, and genetics (40). Again, hemorrhagic shock increased TNK1 expression in both the colon and the small intestine of pigs (Figure 5, F and G).

Apart from SIRS, an apoptotic tissue damage program in the intestine has also been described in chronic IBD (12). Therefore, we examined TNK1 expression in colon and terminal ileum biopsies from patients with severe Crohn's disease (CD) ($n = 6$) and healthy controls ($n = 6$) (Figure 5, H and I). TNK1 expression was increased in biopsies from CD patients as compared with disease controls in both inflamed colon and ileum (Figure 5, H and I). In line with its role to regulate apoptosis in the intestine, the basal level of TNK1 expression was also disrupted in human colon cancer across all stages (Supplemental Figure 4, A and B).

Collectively, our data show that the tight regulation of TNK1 expression is disrupted after severe trauma and intestinal injury

not only under experimental conditions in mice and pigs but also in humans. This suggests that TNK1 is likely to act in a positive-feedback loop to enhance trauma-induced tissue damage.

TNK1 activates NF- κ B and STAT3 signaling to release TNF- α and IL-6. To elucidate the molecular mechanism(s) underlying the TNK1-induced death program, we examined the expression of the proinflammatory cytokines TNF- α and IL-6. Expression of TNK1 resulted in an increase in IL-6 levels in plasma, but also in the colon and duodenum, of TNK1-expressing mice (Figure 6A). In parallel, we detected an increase in TNF- α mRNA in both tissues upon expression of TNK1 (Figure 6B). The TNF- α /IL-6 signaling pathway involves the major transcription factors NF- κ B and STAT3. STAT3 can interact with p65, and together they induce gene transcription (41). Previously it has been shown that TNK1 facilitates TNF- α -induced apoptosis (17) and leads to phosphorylation of STAT1/STAT3 and activation of JAK/STAT signaling (42). Consistent with an increase in TNF- α and IL-6 and in agreement with the previous data, we found robust nuclear staining of phosphorylated STAT3 (p-STAT3) and p65 in TNK1-expressing intestinal epithelium (Figure 6, C and F). Nuclear accumulation of p65 in response to TNK1 expression was validated by examination of p65 expression in nuclear and cytoplasmic fractions, respectively. In the presence of TNK1, there was a marked increase in the amount of p65 protein detectable in the nuclear fraction of intestinal epithelial cells (Figure 6G). Immunoblot analysis confirmed TNK1-induced phosphorylation of STAT3 (Figure 6D), but not of STAT1 or STAT5 (Supplemental Figure 3, E and F). We could further demonstrate that STAT3 phosphorylation is a direct consequence of TNK1 activity using in vitro kinase assays with recombinant STAT3 (Figure 6E). To gain further insight into the molecular signaling events downstream of TNK1, we performed comparative genome-wide transcriptional profiling followed by gene set enrichment analysis. We identified a set of 103 genes in the small intestine that were differentially regulated in TNK1-expressing versus nonexpressing mice (Supplemental Figure 5 and Supplemental Figure 6A). Gene ontology-based classification revealed that genes involved in response to injury or invasive threat are highly represented in the gut of TNK-expressing mice (Supplemental Figure 6B). These results are in line with our observation of intestinal hyperpermeability, bacterial translocation, and a systemic inflammatory response upon expression of TNK1. Furthermore, gene set enrichment analysis of differentially regulated genes revealed that TNK1-expressing mice exhibit a robust gene signature associated with STAT3 and NF- κ B signaling (Supplemental Figure 6C).

Thus, expression of TNK1 results in induction of the TNF- α /IL-6 signaling module in vivo, most likely via activation of the STAT3 and NF- κ B transcription factors.

Blocking TNF- α impairs TNK1-induced intestinal damage. Proinflammatory cytokines (e.g., TNF) are a hallmark of SIRS and also mediate damage in IBD (5, 43). TNF- α is one of the extrinsic signals that initiate apoptosis of enterocytes (44). The apoptosis rate of enterocytes is a determinant of intestinal barrier function. The removal of proinflammatory cytokines from the bloodstream can improve survival in SIRS (5, 13), and TNF- α neutralization represents one of the most efficient biological therapies of IBD. TNK1 facilitates TNF- α -induced apoptosis (17). Our data show that TNK1

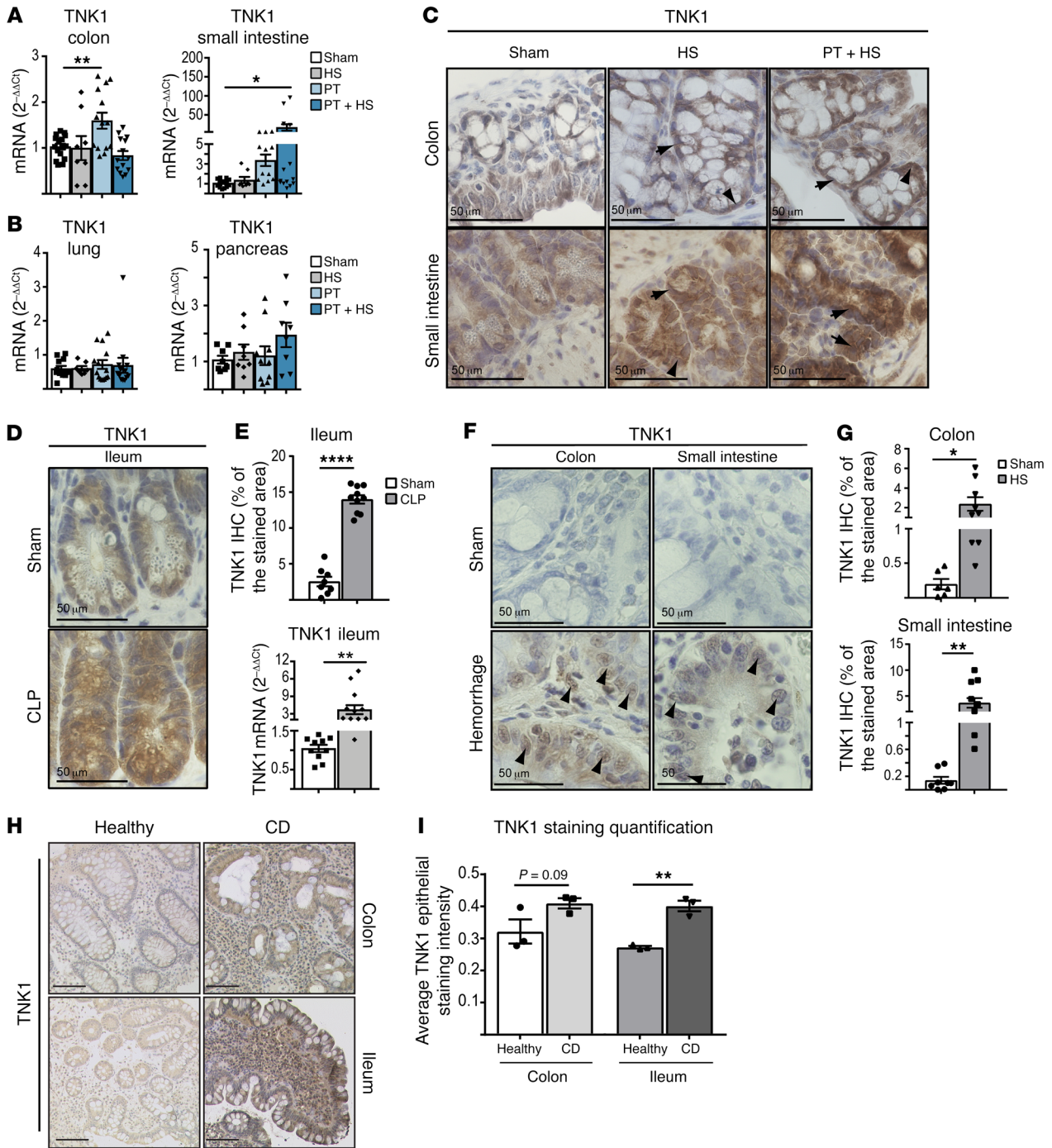


Figure 5. TNK1 expression is dysregulated in response to stress across various species. (A–C) TNK1 is expressed in the small and large intestine in response to polytrauma. Analysis of TNK1 was assessed by RT-qPCR at the mRNA level (A and B) and by immunohistochemistry at the protein level (C) ($n = 10\text{--}12$ per group). HS, hemorrhagic shock; PT, polytrauma. (D and E) TNK1 protein and transcript levels are also increased in the ileal tissue under septic conditions (cecal ligation and puncture [CLP] model). (D) Representative images of ileal sections from CLP mice show increased immunoreactivity for TNK1. (E) Corresponding charts depict quantification of the stained area or TNK1 mRNA level in the ileal tissue of sham and septic mice ($n = 8$ per group). (F and G) TNK1 expression was detectable in the gut of pigs subjected to hemorrhagic shock. Representative images of porcine gut sections stained against TNK1 (F) and corresponding quantification graphs (G) are shown ($n = 6\text{--}8$ per group). (H and I) TNK1 is also elevated in patients suffering from Crohn’s disease (CD) as shown by immunohistochemistry. Representative images (H) and quantification (I) show TNK1 protein expression or its absence in epithelial cells of ileum and colon from healthy individuals and CD patients. Three independent patients per group were investigated, leading to total $n = 6$ per disease state. Data are expressed as mean \pm SEM. Differences were tested by parametric 2-tailed, unpaired Student’s *t* tests. ANOVA test was applied for multiple-comparison analysis. The mean of each column was compared with the mean of a control column by Dunnett’s multiple-comparisons test. ($*P = 0.01\text{--}0.05$; $**P = 0.001\text{--}0.01$; $***P < 0.0001$.) Scale bars: 50 μm (C, D, and F); 100 μm (H).

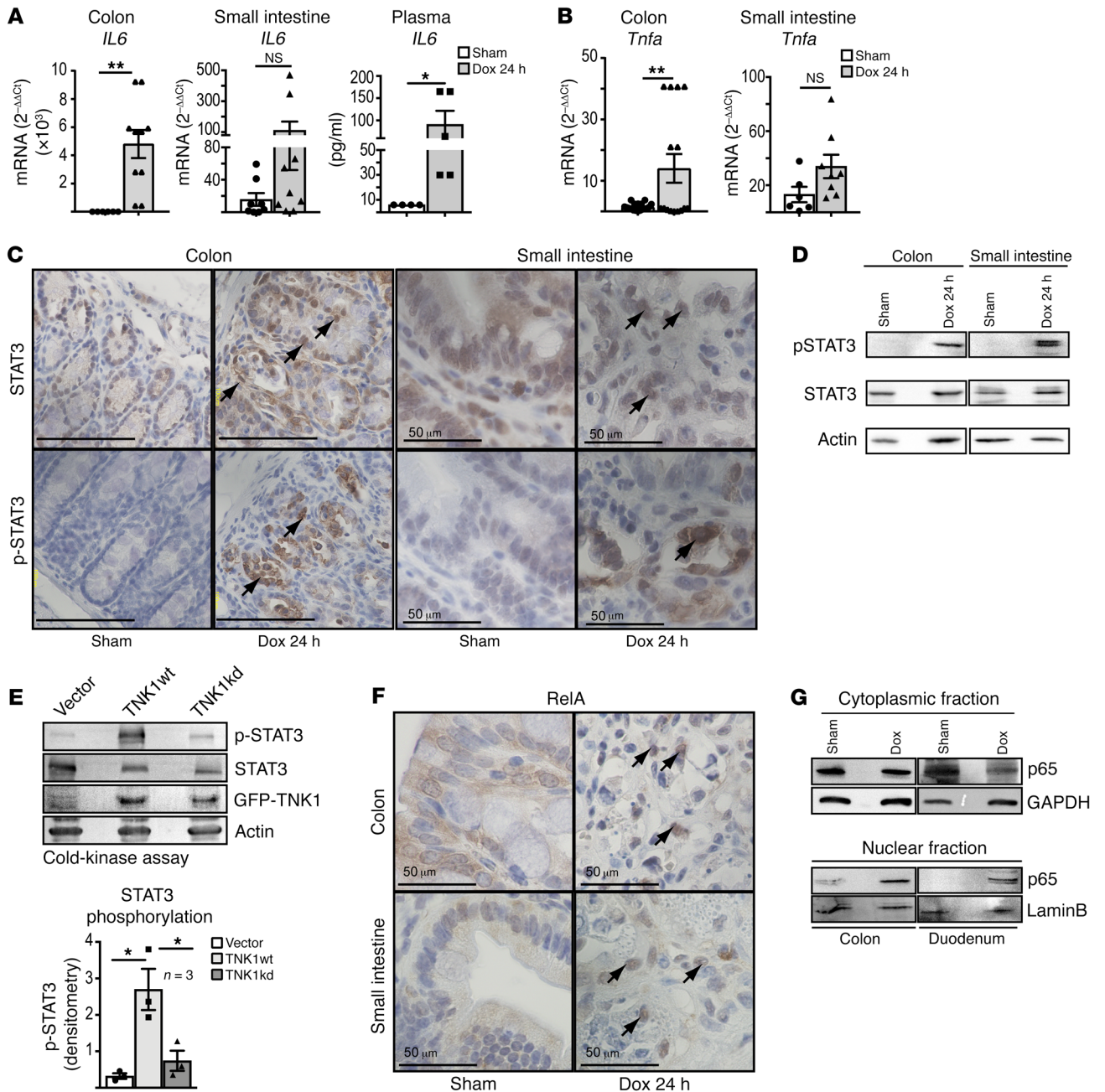


Figure 6. TNK1 expression results in activation of transcription factors STAT3 and NF-κB. (A) Graphs show elevated *IL6* transcript ($n = 8-10$ per group) in the small and large intestine and a massive increase of plasma IL-6 ($n = 5$ per group). (B) Charts show increased levels of *Tnfa* in the colon and small intestine of TNK1-expressing mice ($n = 8-10$ per group). (C-E) TNK1 expression results in phosphorylation and activation of transcription factor STAT3. (C) Representative images of small and large intestine stained for STAT3 and phosphorylated STAT3 (p-STAT3) are shown. Arrows point to nuclear localization of p-STAT3. (D) Representative Western blots show p-STAT3 expression in the small and large intestine 24 hours after TNK1 expression ($n = 3$). (E) STAT3 phosphorylation is a direct consequence of expression of constitutively active TNK1 (TNK1wt) as indicated by *in vitro* kinase assay (wt, wild type; kd, kinase dead) ($n = 3$). (F and G) TNK1 expression also leads to activation and nuclear translocation of NF-κB/p65 subunit. (F) Representative images display nuclear translocation of NF-κB/p65 subunit upon TNK1 expression. (G) Cellular/tissue fractionation shows NF-κB/p65 subunit increase in nuclear fraction upon TNK1 expression ($n = 3$). Arrows point to the nuclear location of p-STAT3 or NF-κB/p65 subunit. Data are expressed as mean \pm SEM. Differences were tested by parametric 2-tailed, unpaired Student's *t* tests. ANOVA test was applied for multiple-comparison analysis. The mean of each column was compared with the mean of a control column by Dunnett's multiple-comparisons test. (* $P = 0.01-0.05$; ** $P = 0.001-0.01$.) Scale bars: 50 μm (C, small intestine, and F), 100 μm (C, colon).

is upregulated in CD and high TNF- α levels are detectable in intestinal tissues upon expression of TNK1 (Figure 5, H and I, and Figure 6B). Therefore, we examined whether therapeutic targeting of TNF- α may prevent apoptotic events and attenuate TNK1-induced

injury of gastrointestinal mucosa. TNK1-expressing mice treated with the anti-TNF- α antibody infliximab (IFX) before doxycycline treatment revealed a more favorable clinical course with significantly lower weight loss and preserved colon length as compared

with mice treated with doxycycline alone (Figure 7, A and B, and data not shown). In line with this clinical outcome, the integrity of the intestinal mucosa appeared improved (Figure 7C). The barrier proteins E-cadherin and claudin-1 were normally distributed at the sites of cell-cell contact in IFX- and doxycycline-treated animals, indicating a virtually intact mucosal architecture (Figure 7D). TNK1 expression (Figure 7C, right) itself was not affected by IFX, suggesting that TNF- α acts downstream of TNK1 in line with the data presented above. To specifically investigate whether anti-TNF- α treatment can limit the TNK1-induced apoptotic program in the gut, immune labeling for cC3 was conducted. Only doxycycline-treated mice showed pronounced apoptosis predominantly at the cryptal base of the colon and small intestine. When mice were pretreated with IFX, the number of apoptotic cells was markedly reduced in TNK1-expressing mice (Figure 7, E and F). Besides, *Lgr5* transcript levels were only slightly diminished in the intestinal crypts of TNK1-expressing mice pretreated with IFX (Figure 7G). Finally, we assessed TNF- α transcript levels in mice treated with IFX and doxycycline versus mice treated with doxycycline only. The previously observed TNF- α induction upon TNK1 expression was either abolished or strongly attenuated in the small intestine and colon, respectively, indicating a feed-forward loop driven by the TNK1/TNF- α axis (Figure 7H).

Loss of TNK1 protects the intestinal mucosa. To additionally prove the pathophysiological relevance and specificity of our model and to exclude that high TNK1 expression levels simply activate an artificial death program, we first reduced the dose of doxycycline in TNK1-expressing mice. Indeed, there is a clear correlation between TNK1 expression levels and the extent of damage in the intestine and thus improved survival of the animals (Supplemental Figure 7, A-F).

Second, a Cre-lox approach (*VilCreTnk1^{-/-}*) was applied to delete *Tnk1* specifically in the intestine (Figure 8A and Supplemental Figure 8). These mice were viable and healthy without any signs of colitis or tumor formation (data not shown). We induced experimental colitis in WT (*Tnk1^{fl/fl}*) or *Tnk1*-knockout (*VilCreTnk1^{-/-}*) mice using dextran sodium sulfate (DSS) as a chemical inducer of epithelial injury, which results in intestinal inflammation. DSS is widely used for this purpose and faithfully recapitulates the features of ulcerative colitis (45).

Epithelial injury inflicted by DSS led to an upregulation of TNK1 expression in WT mice (*Tnk1^{fl/fl}*), further supporting our hypothesis that TNK1 is a central mediator of intestinal damage. As expected, there was no TNK1 expression either in the intestine of *VilCreTnk1^{-/-}* mice or in organoid cultures derived therefrom (Figure 8, B and C, and Supplemental Figure 8). *Tnk1^{fl/fl}* mice exhibited the expected severe inflammation with transmural leukocyte infiltration, thickening of the bowel wall (Figure 8, D, E, and G, and Supplemental Table 1), and a severe loss of goblet cells (Figure 8F). The intestinal barrier appeared disrupted as indicated by a loss of AJs and TJs as determined by immunofluorescence (IF) of E-cadherin and claudin-1, respectively (Figure 8H). In contrast, *VilCreTnk1^{-/-}* mice developed less severe colitis than *Tnk1^{fl/fl}* mice in response to DSS. *Tnk1*-knockout mice exhibited only moderate inflammation as demonstrated by a significantly lower histological bowel inflammation score and a significantly higher number of goblet cells compared with *Tnk1^{fl/fl}* mice (Figure 8, D-G, and Supplemental Table 2). Furthermore, the intestinal barrier appeared

less disturbed in *VilCreTnk1^{-/-}* mice (Figure 8H). Consistently, tissue levels of the proinflammatory cytokines IL-6 and TNF- α in the colon were significantly lower (Figure 8, I and J). These data suggest that TNK1 indeed acts to promote intestinal damage in response to various exogenous stressors.

Discussion

Sepsis and multi-organ failure are serious and frequent complications of trauma, and gut failure is an essential factor in the pathogenesis and progression of systemic inflammation that can culminate in multiple organ failure (MOF). A key pathological event in this process is the failure of the gastrointestinal barrier with resulting translocation of luminal substrates to the bloodstream and loco-regional lymph nodes. This is followed by the exacerbation of local and systemic immune responses. All these events contribute to the pathophysiological crosstalk between the gut, liver, and pancreas as well as distant organs such as the lung. The gut-lymph-lung axis is a direct anatomical link between the gut and the lung. Breakdown of the intestinal barrier leads to the release of nonbacterial, gut-derived factors into the mesenteric lymph, leading to distant organ damage (46, 47). Mesenteric lymph bypasses the portal circulation and consequently the secondary “firewall” provided by the liver. Unfiltered luminal components, locally produced cytokines, and activated immune cells that exit the mesenteric lymph nodes will be able to leak directly to the pulmonary circulation and cause acute lung injury.

Increased intestinal permeability positively correlates with MOF and poor prognosis. Indeed, the breakdown of the intestinal barrier is observed as a secondary event after various acute traumas, e.g., brain injury (48) or severe liver damage (49), but the mechanisms involved are poorly characterized. Pronounced apoptosis is observed in several tissues during MOF, particularly in acute lung injury and AGI. This points to organ-spanning factors that mediate or initiate such a damage program. By nature, such factors require a swift and also tight regulation of their activity (50).

In the current study, we identify TNK1 as a key mediator of intestinal apoptosis in response to various stressors, leading to intestinal damage, a breakdown of the intestinal barrier, increased intestinal permeability, and subsequent multi-organ dysfunction.

TNK1 is a tyrosine kinase whose activity is primarily regulated by expression and not by upstream regulators. Upon expression, the kinase shows almost the maximal activity. This is most likely the reason why its expression is tightly regulated, e.g., during embryonic development. Adult tissues exhibit only a low level of *Tnk1* mRNA (17). Methylation of the *Tnk1* promoter and binding of the transcription factors SP1, SP3, AP2, and MED1 regulate the *Tnk1* promoter in a combinatorial manner, which could account for differential expression of TNK1 observed in various tissues (20). Methylation of the CpG sites in the *Tnk1* promoter is a likely mechanism for the negative regulation of TNK1 expression (19). Methylation may prevent transcription factor SP/MED1 proteins from binding to and activating the *Tnk1* promoter (20). *Tnk1* is ubiquitously expressed at low levels, and cellular stress can upregulate expression (24). Enhancement of SP1, SP3, AP2, and MED1 transcription factors under stress conditions is likely to result in enhanced *Tnk1* promoter activation and induction of *Tnk1/Kos1* (20). Moreover, TNK1 has been shown to exert proapoptotic properties (17).

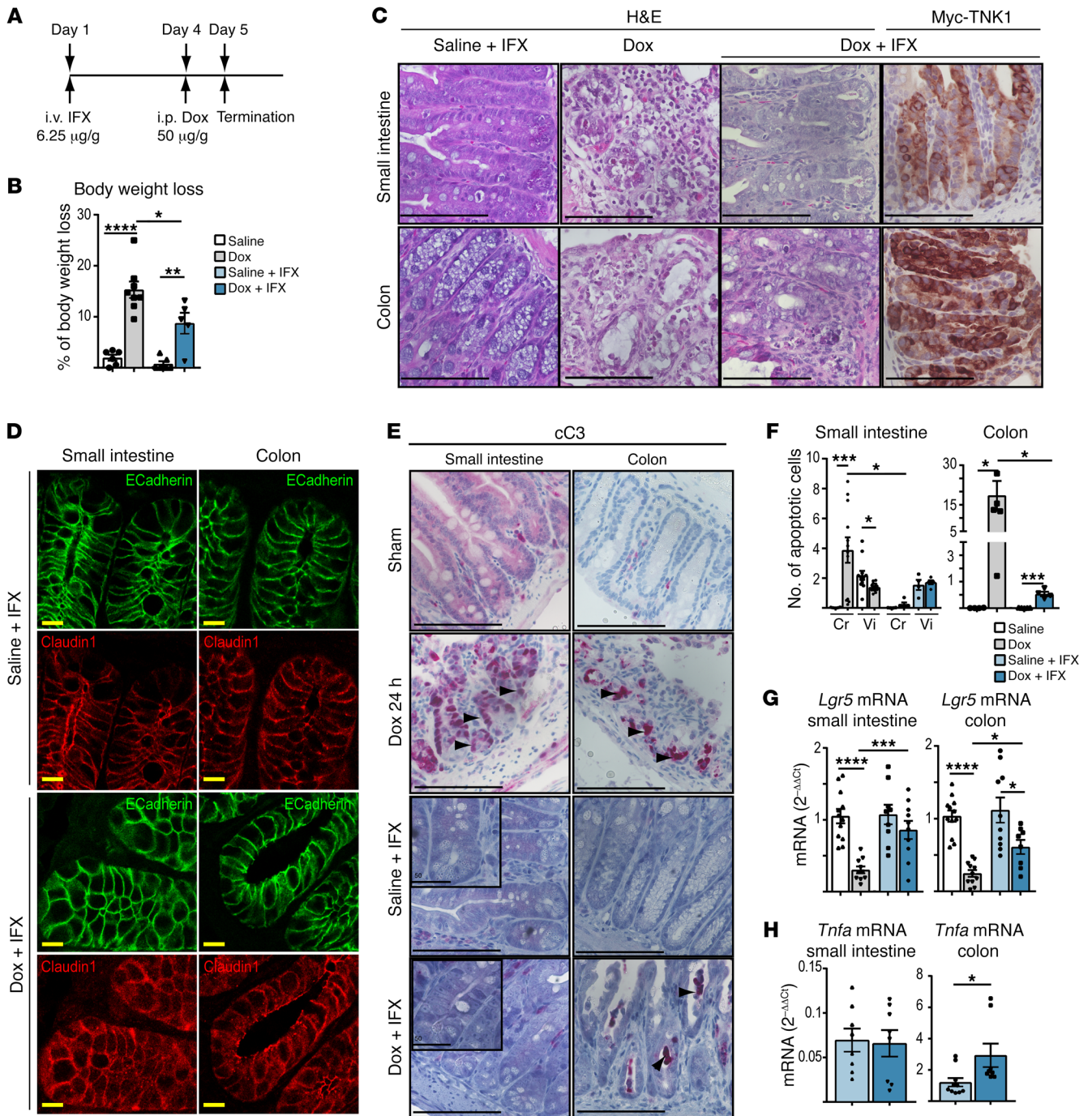


Figure 7. Infliximab abolishes TNK1-induced apoptosis in the small intestine and decreases programmed cell death in the colon. (A) Schematic representation of the infliximab/doxycycline treatment time frame. Infliximab (IFX; 6.25 μ g/g) was administered (day 1) i.v. into the tail vein of 8-week-old animals with matched genotype. Twenty-four hours (day 3) after IFX treatment, doxycycline (Dox; 50 μ g/g) or saline was administered i.p. Mice were sacrificed on the fourth day after the start of the treatment. (B) IFX-pretreated mice revealed an improved clinical picture with a significantly lower weight loss ($n = 6-10$ per group). (C) IFX pretreatment protects architecture of small intestine from the TNK1-induced damage as indicated by H&E staining. Colonic mucosa is only partially preserved under the same treatment condition. The TNK1 expression is not affected by TNF- α neutralization. (D) IFX pretreatment protects intestinal barrier as indicated by the normal distribution of the tight and adherens junction proteins E-cadherin and claudin-1. (E) TNF- α neutralization impairs TNK1-induced apoptosis. Representative images of the murine small and large intestine show immunoreactivity for the apoptotic marker cleaved caspase-3 (indicated by arrowheads). (F) Corresponding charts depict quantification of cell death ($n = 6-10$ per group). Apoptotic cells were counted at the base of the crypt (Cr) and villi (Vi). (G) IFX pretreatment prevents stem cell loss as indicated by RT-qPCR for the stem cell marker LGR5 ($n = 10$ per group). (H) TNF- α induction upon TNK1 expression was strongly attenuated in small intestine and colon ($n = 8-10$ per group). Data are expressed as mean \pm SEM. Differences were tested by parametric 2-tailed, unpaired Student's t tests. ANOVA test was applied for multiple-comparison analysis. The mean of each column was compared with the mean of a control column by Dunnett's multiple-comparisons test. (* $P = 0.01-0.05$; ** $P = 0.001-0.01$; *** $P = 0.0001-0.001$; **** $P < 0.0001$). Scale bars: 50 μ m (E, insets); 100 μ m (C and E); 10 μ m (IF images).

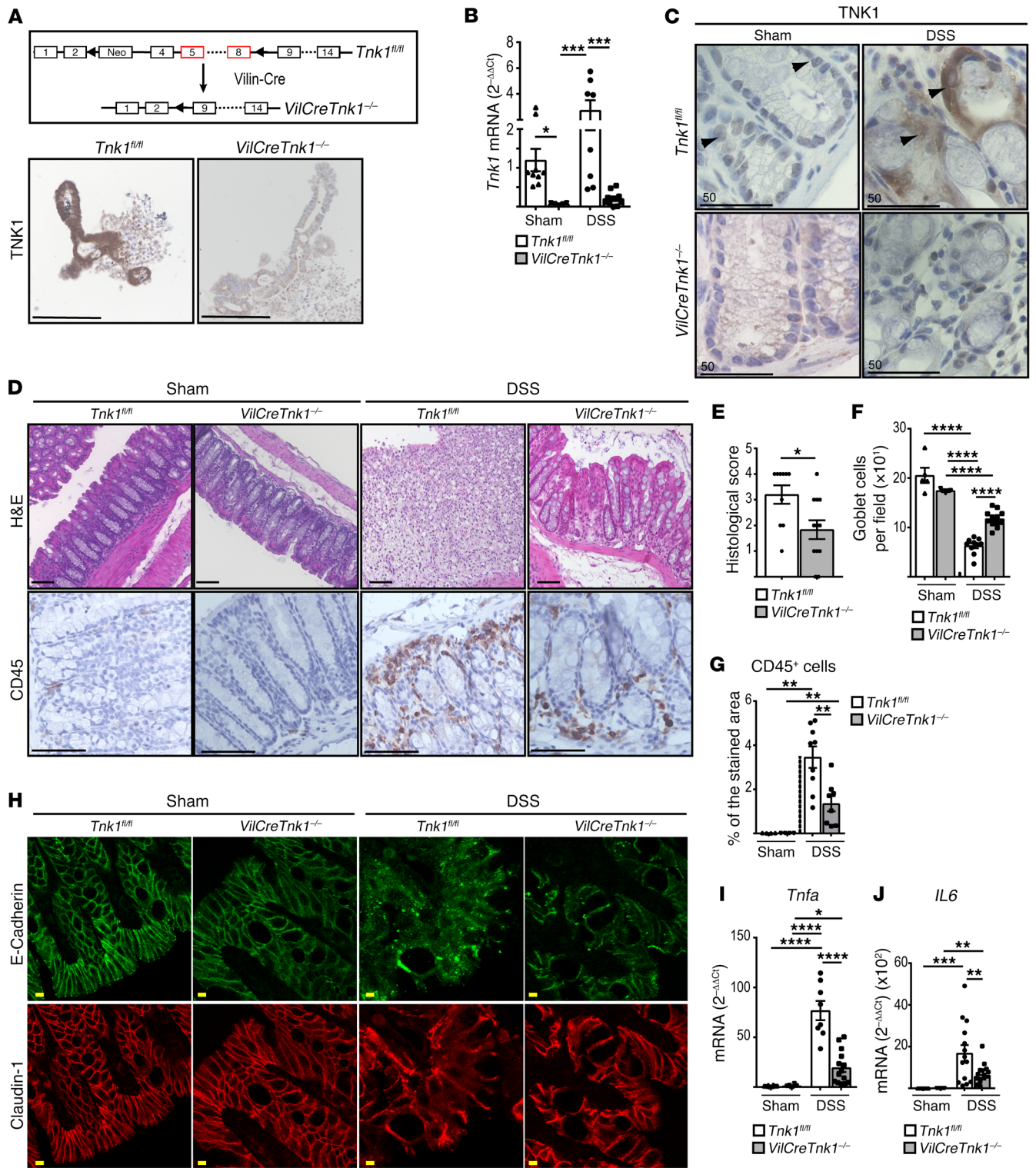


Figure 8. TNK1-deficient mice (*VilCreTNK1^{-/-}*) are less susceptible to DSS-induced colitis. (A) Scheme of the knockout approach. (B and C) TNK1 knockout abolishes TNK1 expression, as shown in mini-gut organoids (A, bottom) and intestine from *VilCreTNK1^{-/-}* mice (mRNA [B] and protein [C]). In response to DSS-induced colitis, *TNK1^{fl/fl}* mice show increased TNK1 expression as compared with untreated *TNK1^{fl/fl}* mice ($n = 8-10$ per group): (B) mRNA and (C) protein. (D) Representative images of H&E-stained colonic sections of *TNK1^{fl/fl}* mice with colitis display increased wall thickness, distortion of the crypt architecture, formation of crypt abscess with the loss of goblet cells, and diffuse infiltration with mononuclear cells. In contrast, sections of *VilCreTNK1^{-/-}* display less severe acute colonic pathology with focal leukocyte infiltration. (E and F) Corresponding graphs represent scoring and grading of inflammation-associated histological changes (E) and quantification of mucin-positive goblet cells (F) ($n = 5-10$ per group). Leukocyte infiltration was confirmed by CD45 staining (D, bottom) and (G) quantification of the stained area ($n = 5-10$ per group). (H) *TNK1^{fl/fl}* mice with colitis show impaired intestinal barrier as indicated by E-cadherin and claudin-1 staining. (I and J) Consistently with the lower histological score, *VilCreTNK1^{-/-}* mice show decreased levels of the proinflammatory cytokines *IL6* and *Tnfa* in colonic tissue ($n = 8-10$ per group). Data are expressed as mean \pm SEM. Differences were tested by parametric 2-tailed, unpaired Student's *t* tests. ANOVA test was applied for multiple-comparison analysis. The mean of each column was compared with the mean of a control column by Dunnett's multiple-comparisons test. (* $P = 0.01-0.05$; ** $P = 0.001-0.01$; *** $P = 0.0001-0.001$; **** $P < 0.0001$.) Scale bars: 50 μm (C); 100 μm (D); 10 μm (IF images).

To further explore the biological function of TNK1, we generated an inducible TNK1 mouse model. In this model, induction of TNK1 resulted in high expression of the kinase in the gut. Upon expression of TNK1, we observed rapid health deterioration and death of the mice. We could exclude cardiovascular or brain injury as a cause of death of the animals since neither heart nor brain showed histological alterations upon TNK1 expression. There was some lung injury upon TNK expression; however, the clinical relevance of the findings was mild, as blood gas analysis revealed normoxia (data not shown). Strikingly, TNK1-expressing mice exhibited an entirely disrupted intestinal barrier due to intestinal apoptosis, as well as coagulopathy, and hypothermia pointing to severe sepsis as the primary cause of death in response to TNK1 induction. TNK1 expression and intestinal apoptosis were accompanied by a marked cytokine release as demonstrated by increased IL-6 and TNF- α levels in the gut and serum of TNK1-expressing mice.

Thus, TNK1 expression in the intestine could be a motor of multi-organ dysfunction. Intestinal dysfunction has been linked to the pathogenesis of SIRS, acute respiratory distress syndrome, acute lung injury, and MODS. Indeed, barrier failure in the stressed gut seems to be a "point zero" for bacterial translocation and systemic spread but also a source of nonmicrobial, proinflammatory, and tissue-damaging factors. Indeed, TNF- α and IL-6 released by the gut contribute to distant organ damage. Although both ways of distant organ injury (bacteria and released factors) may occur hand in hand, they do not necessarily require each other. This underlines the concept of gut-originated sepsis (6). Indeed, a closer examination of the TNK1-expressing mice revealed both bacterial translocation to loco-regional lymph nodes and release of factors known to mediate injuries, such as TNF- α and IL-6. These observations together with the apoptosis-induced breakdown of the intestinal barrier suggest that TNK1 can be a crucial mediator of the gut-originated sepsis. This hypothesis is supported by the

fact that TNK1 was markedly upregulated in the gut in a mouse model of sepsis and also in response to various stressors such as polytrauma, hemorrhagic shock, or DSS-inflicted intestinal epithelial damage. Expression of TNK1 was not only upregulated in murine trauma models but could also be observed in the porcine intestinal epithelium in response to a hemorrhagic shock. Furthermore, patients with CD also exhibit dysregulated levels of TNK1 expression in their colon and ileum mucosa.

Thus, the dysregulated/upregulated TNK1 expression/activation appears to play a role in the pathogenic process of intestinal barrier disruption upon multiple stressors and in various species. Importantly, depletion of TNK1 in mice with intestine-specific *Tnk1* knockout resulted in a markedly reduced release of cytokines and a substantially attenuated intestinal inflammation when challenged with DSS.

We propose TNK1-triggered apoptosis as the primary mechanism of intestinal barrier disruption. The crypt-villus axis exhibited a gradual decrease in sensitivity to TNK1-induced cell death, although the expression of the transgene appeared homogenous. Most apoptotic cells were detectable at the crypt instead of the villus, indicating apoptosis of stem cells. Consequently, intestinal regeneration was markedly impaired and insufficient. Intestinal apoptosis was also accompanied by a massive disruption of adherens and tight junctions in the gut that are both critical for the preservation of normal intestinal epithelial barrier function and key regulators of paracellular epithelial permeability. Loss of cadherins results in accelerated migration of cells along the crypt-villus axis and consequently in perturbed cellular differentiation (51). The loss of adherens junction can further influence the onset of apoptosis (52) and is also likely to contribute to the observed massive apoptosis and mucosal shedding. The adherens junction proteins of the cadherin family are not just required for the mechanical integrity of the intestinal epithelium but are also a prerequisite for the proper maturation of Paneth and goblet cells (51). In agreement with this, TNK1-expressing mice showed a significantly lower number of goblet cells.

In vitro studies have shown that TNK1 facilitates TNF- α -induced apoptosis through negative regulation of the transactivation capacity of NF- κB (17). Consistently, we show that neutralization of TNF- α limits TNK1-induced apoptosis in the gut. The number of apoptotic cells at the stem cell compartment of the gut was also reduced in infliximab-pretreated TNK1-expressing animals. Thus, the TNK1 expression could at least in part explain the positive effect of therapeutic inhibition of TNF- α on the course of sepsis (53).

The transcription factors NF- κB and STAT3 are regulators of life and death decision for cells. Whether NF- κB induction will lead to apoptosis or survival depends both on signals elicited by the death inducers and on cell type (54). Expression of TNK1 in the intestine was accompanied by NF- κB and STAT3 nuclear translocation/activation and expression of NF- κB /STAT3 proapoptotic and prosurvival target genes. Gene Ontology (GO) terms containing, e.g., keywords "immune," "cytokine stimulus," or "defense" were enriched together with gene sets defining IL-6, TNF- α , NF- κB , and STAT3 signaling, further stressing a TNK1 node involving the IL-6/STAT3 and the TNF- α /NF- κB axis. Notably, the *TNK1* promoter regulating the transcription factors SP1 and SP3 can bind upon IL-6 stimulation on the *STAT3* promoter to

form an IL-6-driven SP1/SP3 protein-DNA complex (55). There is also evidence that TNK1 appears downstream of IL-6 signaling, as human airway smooth muscle cells showed TNK1 induction upon treatment with IL-6-sIL-6R (*trans*-signaling) (56). Furthermore, in this study, GO analysis showed a GO pattern similar to the one we have observed in our analysis of the differentially regulated gene in response to TNK1 expression (56). Thus, we believe that TNK1 might be involved in feedback and -forward signaling loops involving the TNF- α /IL-6 signaling module *in vivo*, most likely via activation of the STAT3 and NF- κ B transcription factors.

Morphological signs of apoptosis in the gut of TNK1-expressing mice coincide with upregulation of proapoptotic executor and sensitizing/activating proteins. Sensitizing proteins like BAD bind to the antiapoptotic proteins (MCL1), thereby liberating activator BCL2 family proteins to promote apoptosis (57). Ultimately, whether cells undergo apoptosis depends on the complex interaction of proapoptotic and prosurvival BCL2 family members. Activation of either of the apoptosis executor proteins of the BCL2 family (BAX, BAK) is necessary and sufficient for mitochondrial pathway apoptosis. They trigger the release of apoptogenic factors from the mitochondria into the cytoplasm, thereby leading to caspase activation. Caspases target several strategic components in the NF- κ B pathway and thereby terminate its antiapoptotic activity, e.g., by direct cleavage of NF- κ B-induced antiapoptotic gene products. cIAP and XIAP are cleaved by caspase-3-related caspases, and overexpression of proteolytic products further potentiate apoptosis (58, 59). Notably, our data show caspase-3 activation and robust cleavage of PARP upon TNK1 expression in the intestinal epithelium.

The findings presented here add to our understanding of pathophysiological signaling in the intestine in response to various stressors/traumas and across different models and species. They directly implicate TNK1 in the pathophysiology of intestinal injury in response to various traumas, including polytrauma and hypovolemic and septic shock, and consequently in MODS. Targeting TNK1 in the intestinal epithelium may be a promising therapeutic approach in situations in which the intestinal homeostasis is disturbed.

Methods

Supplemental Methods are available online with this article; <https://doi.org/10.1172/JCI97912DS1>.

TNK1 mouse models and treatment. A Cre-loxP recombination system under control of the villin promoter was used to delete the TNK1 catalytic domain in intestinal epithelial cells (*VilCreTnk1^{-/-}*).

mTnk1 cDNA corresponding to the kinase region was used to screen, by hybridization, a mouse 129/Ola Cosmid genomic library for full-length *mTnk1* genomic DNA. Long arm (exons 3–14) and short arm (exons 1–2) were obtained from *mTnk1* genomic clone MPMGc-121D21266Q2 (RZPD, Berlin) and subcloned into targeting vector (pPNT4). The targeting construct was electroporated into the E14 embryonic stem (ES) cells, and homologous recombination-positive clones were identified by Southern blot. Targeted-ES clones were injected into the blastocyst of a pseudopregnant female (C57BL/6N) to obtain chimeras. Subsequently, chimeras were bred to mice with the C57BL/6N genetic background to assure a germline transmission. Intestine-specific *Tnk1* deletion was achieved by cross-breeding of

homozygote *Tnk1*-floxed animals (*Tnk1^{fl/fl}*) with animals expressing Cre recombinase under the control of the villin promoter.

The Cre-flox-based inducible cassette exchange approach was used to establish an inducible *Tnk1*-knockin mouse model. The *Tnk1*-knockin model is a Tet-On system that bears an inducible tetracycline-responsive promoter element and the active form of TNK1 kinase at the X-chromosomal *Hprt* locus, in addition to a reverse tetracycline-controlled transactivator (rtTA) at the *Rosa26* locus (*Rosa26rtTA*) (60).

Eight-week-old *Tnk1*-knockin mice (*Rosa26rtTA/+*, *Hprt Myc-Tnk1tg*) were injected i.p. with doxycycline (50 μ g/g) to induce expression of TNK1. Control animals were injected i.p. with the same volume of saline solution (0.9% NaCl).

Acute colitis was pharmacologically induced in *Tnk1^{fl/fl}* and *Vil-CreTnk1^{-/-}* mice as previously described (45). Shortly thereafter, mice were fed for 7 days with 4% DSS polymer in drinking water provided ad libitum (1 DSS cycle) and subsequently sacrificed on day 8 (45). The severity of colitis was estimated according to Wirtz et al. (45).

TNF- α neutralization was achieved by infliximab (IFX) pretreatment of *Rosa26rtTA/+*, *Hprt Myc-Tnk1tg/+* mice (6.25 mg/kg IFX, single i.v. injection). Forty-eight hours after IFX pretreatment, animals were exposed to doxycycline (50 μ g/g, i.p.) to induce expression of TNK1. The experiment was terminated 24 hours after doxycycline or saline exposure.

Statistics. Data were expressed as the mean \pm SEM. Differences were tested by parametric 2-tailed, unpaired Student's *t* tests. ANOVA test was applied for multiple-comparison analysis. The mean of each column was compared with the mean of a control column by Dunnett's multiple-comparisons test. The *P* values of less than or equal to 0.05 were considered statistically significant. The Kaplan-Meier method was used to estimate survival probabilities and to compare survival between mouse cohorts. Statistical analysis was done using GraphPad software.

Study approval. All experimental procedures conducted on animals were approved by the Animal Care committee of Ulm University and the federal authorities for animal research (Tübingen, Germany). The experiments were performed in adherence with the German national guidelines for the use of laboratory animals (Deutsche Tierschutzgesetz) and the European Union "Directive 2010/63/EU on the protection of animals used for scientific purposes" (animal experiment approval numbers TVA Nr-1187, TVA Nr-1255, TVA-Nr-1194, O-197, TVA Nr-1087).

Prior to the start of the study, a positive vote from the institutional review board of Ulm University was obtained (approval numbers 317/12, 230/14, 128/15). Participation in the study was voluntary. All patients signed a written informed consent prior to inclusion.

Author contributions

TS, AK, and MA designed the study. TS, AK, and MA conceived the study, supervised all experiments, and evaluated data. AK and TS provided their medical expertise and helped with data evaluation. MA performed most of the experiments, some with support from AKT, CS, AKE, LB, RG, and TFEB. TE assisted with confocal microscopy. PW assisted with electron microscopy. NA performed Western blots. AT, KS, and TB performed histopathological analysis of the tissue sections. DL and SOR contributed to the study of mouse behavior. RH performed ROTEM analysis. MHL provided trauma and septic mouse models and contributed with his expertise in the field of trauma and multiple-organ dysfunction. MA, AK, MRS, and EW generated transgenic mice. AL performed the

RNA array. JMK and HAK performed gene set enrichment analysis. SV measured glucose and corticosterone levels in plasma. KP and SZ generated organoids. SRJ contributed with his expertise in the field of IL-6 signaling. AS performed differential FACS analysis of the bone marrow cell population. BMW provided biopsies from patients. PR provided gut samples from pigs. CW and SB contributed with in situ hybridization. JG performed quantification of TNK1 expression in human gut samples from healthy individuals and Crohn's disease patients. MA, AK, and TS drafted the manuscript. All authors reviewed and approved the final version. TS and AK approved the final version for submission.

Acknowledgments

We thank staff members of the Animal Research Center in Ulm (Tierforschungszentrum-Ulm) for their assistance. We also thank Claudia Längle, Beate Knobel, Kristina Diepold, Sonja Braumueller, and Holger Reim for their skilled technical assistance and Annette Palmer for her expert assistance with animals.

We are grateful to Uwe Knippschild for providing the colon cancer sample library. We thank Franz Oswald and his team for their help with cloning. We also thank Andreas Brey for helpful discussions about TNK1. We thank Michael Kyba for providing A2lox. cre ESCs used for the generation of the TNK1-knockin mouse model. This work was supported by Collaborative Research Center 1149 Project A6 (to AK), DFG grants AZ.96/1-3 (to NA), STE 2467/1-1 (to KS), KL 2544/1-2 (to AK), and EI792/6-1 (to TE); the Forschungskern SyStaR (to AK and TS); Böhringer Ingelheim Ulm University Biocenter (to AK and TS); the NDIMED-Verbund PancChip (to AK); German Cancer Aid (to AK); and the Fritz-Thyssen Foundation (2015-00363 to AK). AK is also an Else-Kröner-Fresenius Excellence Fellow.

Address correspondence to: Thomas Seufferlein, Klinik für Innere Medizin I, Zentrum für Innere Medizin, Albert Einstein Allee 23, 89081 Ulm, Germany. Phone: 49.731.500.44501; Email: thomas.seufferlein@uniklinik-ulm.de.

- Deitch EA. Gut lymph and lymphatics: a source of factors leading to organ injury and dysfunction. *Ann N Y Acad Sci.* 2010;1207(suppl 1):E103–E111.
- Klingensmith NJ, Coopersmith CM. The gut as the motor of multiple organ dysfunction in critical illness. *Crit Care Clin.* 2016;32(2):203–212.
- Piton G, Manzon C, Cypriani B, Carbonnel F, Capellier G. Acute intestinal failure in critically ill patients: is plasma citrulline the right marker? *Intensive Care Med.* 2011;37(6):911–917.
- Strnad P, Tacke F, Koch A, Trautwein C. Liver — guardian, modifier and target of sepsis. *Nat Rev Gastroenterol Hepatol.* 2017;14(1):55–66.
- Zhang H, et al. IL-6 trans-signaling promotes pancreatitis-associated lung injury and lethality. *J Clin Invest.* 2013;123(3):1019–1031.
- Deitch EA. Gut-origin sepsis: evolution of a concept. *Surgeon.* 2012;10(6):350–356.
- MohanKumar K, et al. Intestinal epithelial apoptosis initiates gut mucosal injury during extracorporeal membrane oxygenation in the newborn piglet. *Lab Invest.* 2014;94(2):150–160.
- Matute-Bello G, et al. Soluble Fas ligand induces epithelial cell apoptosis in humans with acute lung injury (ARDS). *J Immunol.* 1999;163(4):2217–2225.
- Ramachandran A, Madesh M, Balasubramanian KA. Apoptosis in the intestinal epithelium: its relevance in normal and pathophysiological conditions. *J Gastroenterol Hepatol.* 2000;15(2):109–120.
- Jilling T, Lu J, Jackson M, Caplan MS. Intestinal epithelial apoptosis initiates gross bowel necrosis in an experimental rat model of neonatal necrotizing enterocolitis. *Pediatr Res.* 2004;55(4):622–629.
- Di Sabatino A, et al. Intraepithelial and lamina propria lymphocytes show distinct patterns of apoptosis whereas both populations are active in Fas based cytotoxicity in coeliac disease. *Gut.* 2001;49(3):380–386.
- Iwamoto M, Koji T, Makiyama K, Kobayashi N, Nakane PK. Apoptosis of crypt epithelial cells in ulcerative colitis. *J Pathol.* 1996;180(2):152–159.
- Bhargava R, et al. Acute lung injury and acute kidney injury are established by four hours in experimental sepsis and are improved with pre, but not post, sepsis administration of TNF- α antibodies. *PLoS One.* 2013;8(11):e79037.
- Vitkus SJ, Hanifin SA, McGee DW. Factors affecting Caco-2 intestinal epithelial cell interleukin-6 secretion. *In Vitro Cell Dev Biol Anim.* 1998;34(8):660–664.
- Yuan DD, et al. Intestinal injury following liver transplantation was mediated by TLR4/NF- κ B activation-induced cell apoptosis. *Mol Med Rep.* 2016;13(2):1525–1532.
- Hoehn GT, et al. Tnk1: a novel intracellular tyrosine kinase gene isolated from human umbilical cord blood CD34⁺/Lin⁻/CD38⁻ stem/progenitor cells. *Oncogene.* 1996;12(4):903–913.
- Azoitei N, Brey A, Busch T, Fulda S, Adler G, Seufferlein T. Thirty-eight-negative kinase 1 (TNK1) facilitates TNF α -induced apoptosis by blocking NF- κ B activation. *Oncogene.* 2007;26(45):6536–6545.
- Lierman E, Van Mieghroet H, Beullens E, Cools J. Identification of protein tyrosine kinases with oncogenic potential using a retroviral insertion mutagenesis screen. *Haematologica.* 2009;94(10):1440–1444.
- Hoare S, Hoare K, Reinhard MK, Lee YJ, Oh SP, May WS. Tnk1/Kos1 knockout mice develop spontaneous tumors. *Cancer Res.* 2008;68(21):8723–8732.
- Hoare S, Hoare K, Reinhard MK, Flagg TO, May WS. Functional characterization of the murine Tnk1 promoter. *Gene.* 2009;444(1–2):1–9.
- Gu TL, Cherry J, Tucker M, Wu J, Reeves C, Polakiewicz RD. Identification of activated Tnk1 kinase in Hodgkin's lymphoma. *Leukemia.* 2010;24(4):861–865.
- Henderson MC, et al. High-throughput RNAi screening identifies a role for TNK1 in growth and survival of pancreatic cancer cells. *Mol Cancer Res.* 2011;9(6):724–732.
- May WS, Hoare K, Hoare S, Reinhard MK, Lee YJ, Oh SP. Tnk1/Kos1: a novel tumor suppressor. *Trans Am Clin Climatol Assoc.* 2010;121:281–292; discussion 293.
- Hoare K, Hoare S, Smith OM, Kalmaz G, Small D, Stratford May W. Kos1, a nonreceptor tyrosine kinase that suppresses Ras signaling. *Oncogene.* 2003;22(23):3562–3577.
- Weidgard CE, et al. TBX3 directs cell-fate decision toward mesoderm. *Stem Cell Reports.* 2013;1(3):248–265.
- York JMI, Blevins NA, McNeil LK, Freund GG. Mouse short- and long-term locomotor activity analyzed by video tracking software. *J Vis Exp.* 2013;(76):50252.
- Remick DG, Xia H. Hypothermia and sepsis. *Front Biosci.* 2006;11:1006–1013.
- Ogura H, et al. SIRS-associated coagulopathy and organ dysfunction in critically ill patients with thrombocytopenia. *Shock.* 2007;28(4):411–417.
- Groschwitz KR, Hogan SP. Intestinal barrier function: molecular regulation and disease pathogenesis. *J Allergy Clin Immunol.* 2009;124(1):3–20.
- Umar S. Intestinal stem cells. *Curr Gastroenterol Rep.* 2010;12(5):340–348.
- Schepers AG, Vries R, van den Born M, van de Wetering M, Clevers H. Lgr5 intestinal stem cells have high telomerase activity and randomly segregate their chromosomes. *EMBO J.* 2011;30(6):1104–1109.
- Barker N, et al. Identification of stem cells in small intestine and colon by marker gene Lgr5. *Nature.* 2007;449(7165):1003–1007.
- Takeda N, Jain R, LeBoeuf MR, Wang Q, Lu MM, Epstein JA. Interconversion between intestinal stem cell populations in distinct niches. *Science.* 2011;334(6061):1420–1424.
- Metcalf C, Kljavin NM, Ybarra R, de Sauvage FJ. Lgr5⁺ stem cells are indispensable for radiation-induced intestinal regeneration. *Cell Stem Cell.* 2014;14(2):149–159.
- Goodman ZD. Grading and staging systems for inflammation and fibrosis in chronic liver diseases. *J Hepatol.* 2007;47(4):598–607.
- Ishak K, et al. Histological grading and staging of chronic hepatitis. *J Hepatol.* 1995;22(6):696–699.

37. Denk S, et al. Role of hemorrhagic shock in experimental polytrauma. *Shock*. 2018;49(2):154–163.
38. Rittirsch D, Huber-Lang MS, Flierl MA, Ward PA. Immunodesign of experimental sepsis by cecal ligation and puncture. *Nat Protoc*. 2009;4(1):31–36.
39. Knöller E, et al. Effects of hyperoxia and mild therapeutic hypothermia during resuscitation from porcine hemorrhagic shock. *Crit Care Med*. 2016;44(5):e264–e277.
40. Calzia E, Huber-Lang M, Ignatius A, Radermacher P, Thiemermann AC. Modeling traumatic-hemorrhagic shock — nothing is simple and easy. *Shock*. 2012;38(6):685–686.
41. Grivennikov SI, Karin M. Dangerous liaisons: STAT3 and NF-kappaB collaboration and crosstalk in cancer. *Cytokine Growth Factor Rev*. 2010;21(1):11–19.
42. Ooi EL, et al. Novel antiviral host factor, TNK1, regulates IFN signaling through serine phosphorylation of STAT1. *Proc Natl Acad Sci U S A*. 2014;111(5):1909–1914.
43. Duprez L, et al. RIP kinase-dependent necrosis drives lethal systemic inflammatory response syndrome. *Immunity*. 2011;35(6):908–918.
44. Fries W, et al. Infliximab and etanercept are equally effective in reducing enterocyte APOPTOSIS in experimental colitis. *Int J Med Sci*. 2008;5(4):169–180.
45. Wirtz S, Neufert C, Weigmann B, Neurath MF. Chemically induced mouse models of intestinal inflammation. *Nat Protoc*. 2007;2(3):541–546.
46. Caty MG, Guice KS, Oldham KT, Remick DG, Kunkel SI. Evidence for tumor necrosis factor-induced pulmonary microvascular injury after intestinal ischemia-reperfusion injury. *Ann Surg*. 1990;212(6):694–700.
47. Koike K, Moore EE, Moore FA, Read RA, Carl VS, Banerjee A. Gut ischemia/reperfusion produces lung injury independent of endotoxin. *Crit Care Med*. 1994;22(9):1438–1444.
48. Stanley D, et al. Translocation and dissemination of commensal bacteria in post-stroke infection. *Nat Med*. 2016;22(11):1277–1284.
49. Pijls KE, Koek GH, Elamin EE, de Vries H, Masclee AA, Jonkers DM. Large intestine permeability is increased in patients with compensated liver cirrhosis. *Am J Physiol Gastrointest Liver Physiol*. 2014;306(2):G147–G153.
50. de Santa Barbara P, van den Brink GR, Roberts DJ. Development and differentiation of the intestinal epithelium. *Cell Mol Life Sci*. 2003;60(7):1322–1332.
51. Schneider MR, et al. A key role for E-cadherin in intestinal homeostasis and Paneth cell maturation. *PLoS One*. 2010;5(12):e14325.
52. Hermiston ML, Gordon JL. In vivo analysis of cadherin function in the mouse intestinal epithelium: essential roles in adhesion, maintenance of differentiation, and regulation of programmed cell death. *J Cell Biol*. 1995;129(2):489–506.
53. Qiu P, Cui X, Barochia A, Li Y, Natanson C, Eichacker PQ. The evolving experience with therapeutic TNF inhibition in sepsis: considering the potential influence of risk of death. *Expert Opin Investig Drugs*. 2011;20(11):1555–1564.
54. Kaltschmidt B, Kaltschmidt C, Hofmann TG, Hehner SP, Droge W, Schmitz ML. The pro- or anti-apoptotic function of NF-kappaB is determined by the nature of the apoptotic stimulus. *Eur J Biochem*. 2000;267(12):3828–3835.
55. Loeffler S, Fayard B, Weis J, Weissenberger J. Interleukin-6 induces transcriptional activation of vascular endothelial growth factor (VEGF) in astrocytes in vivo and regulates VEGF promoter activity in glioblastoma cells via direct interaction between STAT3 and Sp1. *Int J Cancer*. 2005;115(2):202–213.
56. Robinson MB, et al. IL-6 trans-signaling increases expression of airways disease genes in airway smooth muscle. *Am J Physiol Lung Cell Mol Physiol*. 2015;309(2):L129–L138.
57. Thomas LW, Lam C, Edwards SW. Mcl-1; the molecular regulation of protein function. *FEBS Lett*. 2010;584(14):2981–2989.
58. Clem RJ, et al. c-IAP1 is cleaved by caspases to produce a proapoptotic C-terminal fragment. *J Biol Chem*. 2001;276(10):7602–7608.
59. Deveraux QL, Leo E, Stennicke HR, Welsh K, Salvesen GS, Reed JC. Cleavage of human inhibitor of apoptosis protein XIAP results in fragments with distinct specificities for caspases. *EMBO J*. 1999;18(19):5242–5251.
60. Kyba M, Perlingeiro RC, Daley GQ. HoxB4 confers definitive lymphoid-myeloid engraftment potential on embryonic stem cell and yolk sac hematopoietic progenitors. *Cell*. 2002;109(1):29–37.
61. Buczacki SJ, et al. Intestinal label-retaining cells are secretory precursors expressing Lgr5. *Nature*. 2013;495(7439):65–69.